

Qualitative Laser-Induced Incandescence Measurements of Soot Emissions During Transient Operation of a Port Fuel-Injected Engine

Peter O. Witze

*Combustion Research Facility
Sandia National Laboratories
Livermore, California, USA*

To appear in proceedings of
*The Fifth International Symposium on Diagnostics and Modeling
of Combustion in Internal Combustion Engines
COMODIA 2001
July 1-4, 2001, Nagoya, Japan*

ABSTRACT

Beginning in 2004, all passenger cars and light-duty trucks sold in the U.S. will be required to meet the same emission regulations regardless of the fuel type (EPA Tier 2). Thus, for the first time gasoline-fueled vehicles will have to meet particulate matter emission standards that in the past have only been required of diesel-fueled vehicles. It is expected that contemporary port fuel-injected (PFI) engines with catalysts will be able to meet the requirements, which are currently based on particulate mass. In contrast, it is uncertain at this time whether the new generation of direct-injection gasoline engines can achieve certification. Furthermore, health risks are more strongly correlated with particle size and number density than with mass concentration. If new regulations are based on these parameters, gasoline engines will come under closer scrutiny.

To help meet these new and anticipated regulations, improved particulate measurement techniques are needed. The two capabilities most urgently required are fast response to follow transients, and high-sensitivity to measure small amounts in short times. Laser-induced incandescence (LII) offers these capabilities.

The purpose of this paper is to demonstrate the use of LII for making time-resolved measurements of soot volume fraction during engine transients. The measurements presented were made at the exhaust-port exit of a production, four-valve, PFI spark-ignition engine with only one active cylinder. Optical access to the exhaust flow between the head and exhaust manifold was achieved by an optical flow channel with three windows, which permitted a laser beam to cross the exhaust stream while observed from above. Planar LII imaging was used to investigate the spatial distribution of soot across the exhaust port; analog LII measurements were made to measure the soot volume fraction during transient engine operation.

The planar LII images obtained in the exhaust port show that soot concentration varies widely both spatially and temporally, from cycle-to-cycle. For some cycles the soot distribution was relatively uniform, whereas for others it varied greatly between the two valves. On average, the amount of soot emitted from each valve was different.

For open-valve injection, the soot volume fraction increased rapidly over the first 20 cycles of a simulated cold start, and then continued to increase at a slower rate for the duration of the 300 cycle test. In contrast, for closed-valve injection the soot volume fraction rose very quickly to a maximum in less than 10 cycles, and then fell rapidly to a low concentration by about 50 cycles, after which it continued to fall gradually for the remainder of the test. We believe the large differences in the soot behavior for these two cases is related to the dynamics of the in-cylinder wall films, and in particular, to the changing composition of the films as wall temperatures increase.

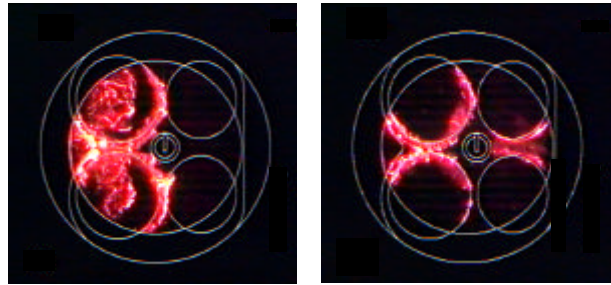
For a snap-throttle transient, where the manifold pressure was suddenly increased from 40 to 98 kPa, the soot volume fraction increased steadily during the throttled period, fell to near zero at the time of the snap-throttle, and then increased steadily to a value approximately ten times greater than for the throttled period. Severe window fouling occurred during the wide-open-throttle portion of this test, resulting in a 30% loss in laser beam transmission after engine shutdown. This fouling problem limited this study to qualitative observations, and represents the main disadvantage of optical techniques for engine exhaust studies. Fortunately, it is a design problem that can be corrected, although at the expense of added complexity.

INTRODUCTION

Port-fuel-injected gasoline engines exhibit considerably higher levels of soot contamination in the engine oil than do carbureted engines. Quader [1] points out that soot is known to form in rich flames when the equivalence ratio exceeds 1.5, a condition that may occur in spark-ignition engines because of poor fuel distribution or incomplete vaporization that leads to droplet burning. These conditions are particularly prevalent during cold start and at heavy loads. Kosowski [2] showed, using conventional measurement procedures, that the mass of soot emitted from PFI engines is very low. However, a recent air quality study mandated by the Colorado legislature [3] found that light-duty gasoline engines were the source of 75% of the mass of atmospheric carbon particulate matter smaller than 2.5 micron ($PM_{2.5}$) emitted from mobile sources. This percentage was 3 times the amount emitted by diesel engines. (This large disparity is due to the far greater number of gasoline engines, and is not suggesting that diesel engines are cleaner.) While the major source was poorly-maintained "smoker" gasoline engines, the number two source was contemporary gasoline engines during cold start. Conventional soot measurements like those made by Kosowski are insensitive to the submicron particles emitted from a PFI engine. Baumgard and Johnson [4] have shown that a contemporary, visually "clean" heavy-duty diesel engine will produce 3-4 orders of magnitude more small particles than its "smoking" predecessor. A non-smoking diesel engine thus still emits PM that is a health risk because of its small size and large numbers. However, gasoline engines can also produce large numbers of particles in the submicron size range, which is outside the size range that can be seen by eye.

For PFI gasoline engines during cold start, the droplet burning mentioned by Quader [1] is only partially responsible for rich mixture combustion; wall films may play a much more important role. Witze and Green [5] found that in-cylinder fuel films on cold walls do not fully vaporize during combustion, but instead accumulate over many cycles. As the engine warms, the lighter components of the film vaporize, leaving a film of increasingly heavy composition; eventually, the wall reaches a temperature where the film fully vaporizes. During this film-evolution process, it is possible to achieve a gas temperature and mixture strength condition that leads to ignition of the wall film, creating a diffusion-controlled "pool fire" that can persist well past the normal combustion event, as shown in Fig. 1. These images were produced from a color video of the natural emissions from soot in the pool fires. Although it is not possible to explicitly distinguish between pool fires on the head and piston surfaces, it is evident from the pool fire shapes that the intake valve seats are a principal location for wall film accumulation.

The existence of soot from pool fires in PFI engines was first reported by Nogi et al. [6,7] and Ohyama et al. [8], who measured combustion emissions transmitted by an optical fiber in the spark plug. For open-



a.) Closed-valve injection b.) Open-valve injection

Fig. 1 Pool fire images of gasoline wall films during a simulated cold start, observed through a window in the piston (from Witze and Green [5]).

valve injection, they found a radiation intensity increase late in the cycle near a wavelength of 700 nm, which they interpret to be due to diffusion-controlled burning of fuel films on the walls; this correlated with a strong increase in hydrocarbon emissions. Ohyama et al. [9] reported flame images recorded under cold conditions that clearly show burning fuel droplets following passage of the normal flame, and fuel films burning brightly in the post combustion gases. Finally, Song et al. [10] used IR-radiation imaging to infer the presence and burning of liquid films in a PFI engine. Fuel-rich local pockets were observed to begin burning during the normal flame propagation period, and to persist far past the end of normal combustion. For a 75 °C coolant temperature, they detected burning films in the region of the intake valve seats similar to those shown in Fig. 1, while at room temperature they also detected films on the spark plug, squish area, and exhaust valve.

The occurrence and persistence of a pool fire requires excess oxygen to sustain combustion as the wall film vaporizes. The conditions used by Witze and Green [5] to create the pool fires shown in Fig. 1 were not representative of cold starting a production PFI engine, because fuel enrichment was not used. Rather, a stoichiometric mixture was delivered to the engine. Since a significant portion of the fuel is manifest as wall films, the vapor-phase mixture is lean and thus amenable to pool fires. In contrast, for a production-engine cold start, where enrichment is used in an attempt to achieve a stoichiometric vapor-phase mixture, both the occurrence and degree of pool fires will be greatly reduced; similar conditions can be expected for warm, transient conditions as well. Finally, Stevens and Steeper [11] have shown that soot emissions from pool fires on the piston surface may be a significant problem for direct-injection spark-ignition engines running lean at light-load conditions.

Kayes and Hochgreb [12] have proposed a model for particulate matter formation in spark ignition engines that suggests that burning liquid fuel is the major source of soot emissions; however, this mechanism has never been directly confirmed because of the lack of a suitable measurement technique. The very small size of this PM, estimated to have a mean diameter of about 50 nm, requires high sensitivity not found in conventional gravimetric and smoke meter techniques. The state-of-

the-art instrument for measuring soot size distribution, the scanning mobility particle sizer (SMPS), requires about one minute to complete a measurement. Kayes et al. [13] used an SMPS in a fixed-size mode to obtain measurements during start-up and transient operation; by repeating the tests for different sizes, an ensemble size distribution was created. However, because of the very chaotic behavior of pool fires (e.g., they have been observed to occur in alternate cycles [5]), it is desirable to obtain measurements on a cycle-resolved basis. In this paper, we demonstrate how laser-induced incandescence (LII) can achieve this goal.

LASER-INDUCED INCANDESCENCE

LII has become a widely used diagnostic for the investigation of soot in combustion systems ranging from fundamental burners [14-16] to practical devices such as diesel engines [17-19]. Unique features of the technique are its apparent simplicity and excellent sensitivity, estimated by Wainner and Seitzman [20] to be better than one part per trillion ($\sim 2 \mu\text{g}/\text{m}^3$). The measurement is essentially instantaneous, requiring just a fraction of a microsecond. However, the measurement frequency is limited by the repetition rate of a high-power pulsed laser (typically 10-30 Hz, which corresponds to one measurement per engine cycle at 1200-3600 rpm). While it thus is not possible to obtain crank-angle resolution in real-time, ensemble-averaging for many engine cycles can be used to reconstruct transient behavior. Eckbreth [21] discovered the LII phenomenon, and Dec et al. [17] were the first to use the technique for qualitative imaging of soot distribution during diesel combustion. LII has been applied extensively as a diagnostic tool in stationary burners.

The principle behind LII is straightforward: a pulsed laser is used to heat soot particles to their vaporization temperature; because increased laser fluence (energy flux) cannot raise the particle temperature further, and yet only marginally reduces the particle size, a plateau is reached for which the gray-body radiation from the heated particle is independent of laser fluence and proportional to the soot volume fraction (i.e., the product of the number of particles and their mean-diameter cubed). Nature, of course, is never this simple; the particle size change from vaporization is significant [22], and Vander Wal and Choi [23] have shown that morphological changes may occur due to laser heating that affect its absorptivity. Considering the complexity of engine soot and its measurement, these are not considered overwhelming problems.

LII has a well-defined but complex response to volatile particulate matter. It is totally insensitive to liquid particles, because they absorb a negligible amount of laser energy compared to carbon. For carbon particles coated with volatile material, the latter will vaporize very early in the LII laser-heating period, yielding a volume-fraction measurement that can be significantly smaller than measured, for example, by the SMPS. In general, it is reasonable to state that LII measures the volume fraction of carbonaceous material in the exhaust.

EXPERIMENTAL SETUP

This study was performed on the same experimental engine used to create Fig. 1, a production, 1994 General Motors Quad 4 mounted on a single-cylinder block. To obtain optical access to the exhaust flow, the spacer block diagrammed in Fig. 2 was installed between the head and exhaust manifold. An optical flow channel mounted within this spacer was aligned with the active, #3 exhaust port. The channel was removable for ease of window cleaning, or replacement with a non-optical version when windows were not required. As indicated by the arrows, the laser beam entered the spacer from below, turned by a mirror to pass horizontally through the flow channel, and then turned by a second mirror to dump into the passive #4 exhaust port.

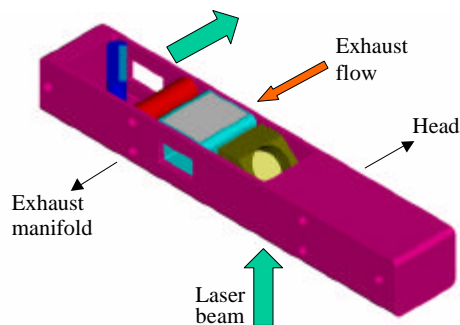


Fig. 2 Spacer block used to obtain optical access to the exhaust port of the active cylinder.

The optical flow channel is shown in Fig. 3. It has two square, opposed side windows for passage of the Nd-YAG laser beam (second harmonic at 532 nm), and a larger rectangular window on the top. For the planar imaging investigation, the laser sheet crossed the channel at a 45-degree angle to the flow direction, and was observed by an intensified CCD camera positioned normal to the sheet, corresponding to View 2. For the analog LII measurements, the 7 mm diameter, collimated beam of the laser was used directly, centered on the square windows. The photomultiplier tube was positioned directly above the beam, and an 8 mm length of

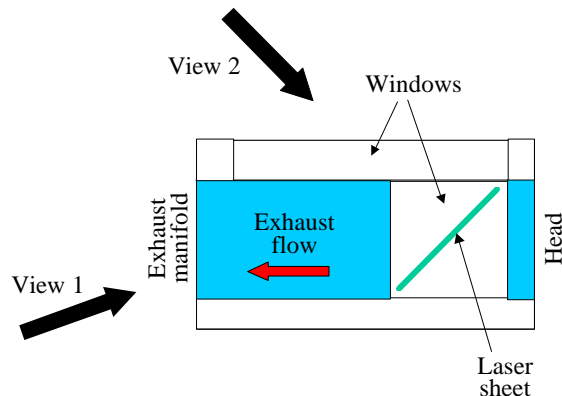


Fig. 3 Schematic diagram of the optical flow channel, showing the orientation of the laser sheet and the camera views for images to be presented in Figs. 4 (View 1) and 5 (View 2).

the beam (approximately) at mid-channel was imaged onto the detector.

Figure 4 contains photographs (View 1 in Fig. 3) showing the status of the optical flow channel following several cold start tests under rich conditions (although similar fouling occurred for the stoichiometric snap-throttle test sequence). In the lower center of (a) the septum dividing the two exhaust ports is just barely visible. It is evident from the soot-deposit pattern on the top window that there is a jet-like flow from the valves during at least a part of the exhaust process. Note that the size of the deposit region on the left is larger than the one on the right. LII imaging results to be presented in the following figure support this observation.

The circular regions on the two side windows are the “burn spots” where the laser beam has vaporized the soot deposits. The pattern on the entrance window on the right side is shown enlarged in Fig. 4b. The dark regions within the spot are indicative of the spatial profile of the beam intensity. The black region in the center of the window, just outside the burn spot, is a crack in the window that was caused by the focused laser sheet used to obtain the LII images.

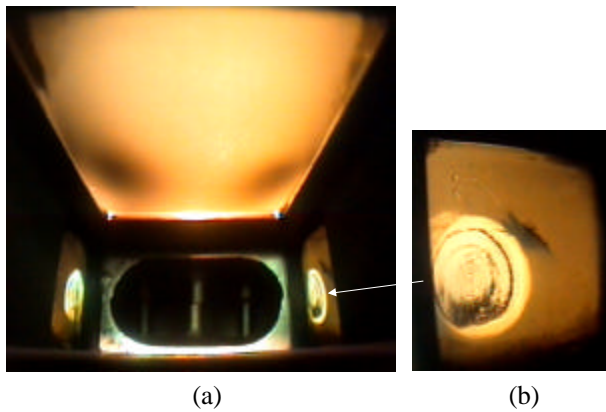


Fig. 4 Photographs showing the soot patterns on the three windows.

IMAGING RESULTS

Because of the non-repeatability of an actual cranking start, we chose to emulate the cold start procedure described by Fox et al. [24], where the engine is motored at constant speed with the ignition system active. Fuel injection is initiated using a with a fixed duration pulse (i.e., no transient enrichment). We chose a high-speed-idle condition of 1200 rpm for compatibility with the 10 Hz pulse rate of the laser. We used an initial coolant temperature of 40° C to minimize the number of misfires at the start of injection. Finally, because of high background noise from fouled windows, it was necessary to use a rich mixture of equivalence ratio $\phi=1.24$ to obtain suitable images. Background subtraction was employed, using the image from the last motored cycle prior to the start of injection.

Shown in Fig. 5 are LII images of the soot distribution across the exhaust port for View 2 in Fig. 3. The numbers under the images indicate the cycle number of the simulated cold start sequence. Early in the test se-

quence, very little soot was observed. The image for cycle 80 was selected for presentation because of the very large “droplet” that was captured. Its indicated diameter is about 5 mm, which is physically unlikely and therefore probably enhanced by blooming from saturation of the CCD pixels. It is also unclear as to the physical source of the light emitted from the droplet. It could be intense elastic scattering leaking through the long wave pass filter, or it could be laser-induced fluorescence (LIF) from fuel or oil in the droplet.

Cycles 116, 140, and 161 were selected for presentation as representative of nearly homogeneous soot distributions of different concentrations, illustrating the large variations from cycle-to-cycle that were observed. The image for cycle 116 is probably most representative of the laser intensity distribution across the sheet. Although the spatial profile of this laser beam is closer to being “top hat” than Gaussian, a planar sheet formed from a circular beam still has strong lateral gradients in intensity.

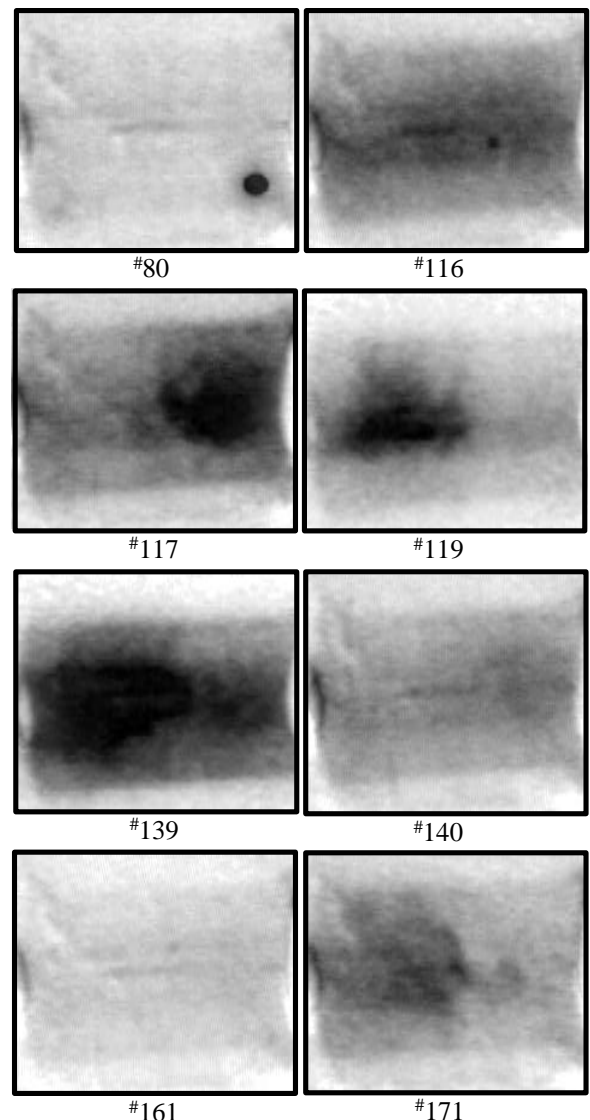


Fig. 5 Planar LII images of soot distributions across the exhaust flow.

Finally, cycles 117, 119, 139, and 171 were selected to illustrate the large inhomogeneities observed in the spatial distributions of the soot, and the propensity for the port on the left side to produce more soot than the one on the right. We believe that simultaneous imaging of liquid films and/or pool fires in the cylinder will reveal a distinct correlation with these patterns of soot distribution.

ANALOG LII SIGNAL PROCEDURES

During steady-state operation, the soot concentration in the exhaust flow is reasonably constant, such that the 8-bit resolution of the digital storage scope used for data acquisition (500 MHz bandwidth, 5 GS/s digitization rate) is sufficient for the dynamic range encountered in the LII signals. In addition, the scope can be operated in an averaging mode, for which the output is 16-bit. However, for single, successive cycle measurements this resolution is inadequate. To remedy this we connect the photomultiplier output to three channels of the scope, set for sensitivities of 1, 5, and 25 mv/division. This, however, alters the termination impedance of the signal, which is optimized for 50 ohms. In Fig. 6 we compare an LII measurement for the three split signals (for a single sensitivity setting) with that of a single, properly terminated signal. The coincidence of the three split signals requires identical cable lengths for each channel. If the channels are simply "daisy-chained" (i.e., connecting to the first, then from there to the second, etc.), both the waveform and temporal response of each channel will be different. Properly split, the temporal response of the three signals is identical but retarded, and beyond 30 ns (not shown) the signals oscillate wildly due to line reflections. By specifying the LII measurement to be the area above the signal for the 30 ns interval shown, we avoid the oscillations and, in essence, calibrate-out the temporal response perturbation as a systematic error.

LII DURING COLD START

Because it is possible to make only one LII measurement each engine cycle at 1200 rpm, we wanted to determine the optimum crank-angle in the exhaust stroke for making the measurement. We did this by making "pseudo" cycle-resolved measurements, where the acquisition angle was incremented by one crank-angle degree (CAD) each cycle, as shown in Fig. 7. Unfortunately, because of the severe window fouling problem discussed earlier, we could not wait for the engine to reach steady state to perform this test. We probably would have had difficulty detecting a low soot concentration through a dirty window. However, although these measurements were carried out for a transient sequence, they clearly reveal the blowdown process at about 150 CAD, which is in good agreement with exhaust-valve-opening at 142 CAD. Based on this result, we chose to make all further measurements at 200 CAD.

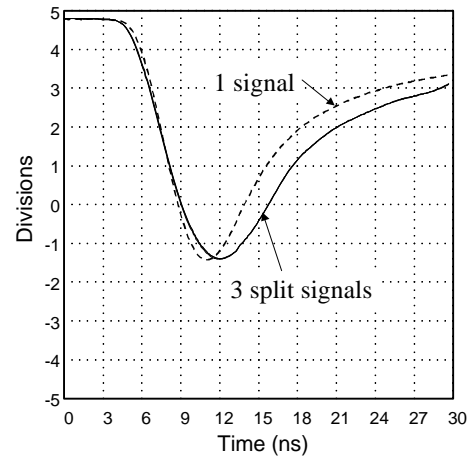


Fig. 6 Comparison between single and multiple PMT records.

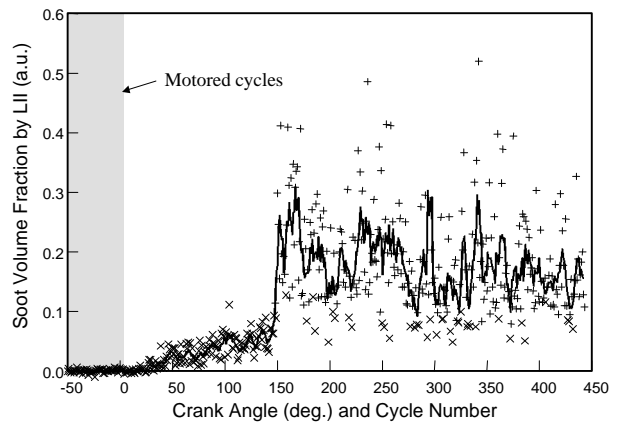


Fig. 7 LII measurements obtained at incremental crank-angle positions during a fueling start. The symbols indicate the single-cycle measurements (\times for data from the first, most sensitive channel of the digital recorder, $+$ for the second channel, and \times again for the third), and the solid line represents a sliding average of five measurements.

Presented in Fig. 8 are data for a 300 cycle, cold start sequence with open-valve injection; we chose to use an equivalence ratio of $\phi=1.24$ for compatibility with Fig. 5. The background LII signal subtracted from the measurements was calculated from the average of the 50 motored cycles at the start of the test sequence. Soot was not detected at the onset of combustion (the engine typically was firing by the fifth cycle), but instead increased monotonically over the first 20 engine cycles. Beyond this point, the data assume a new slope that is lower and nearly constant for the remainder of the test sequence. This second regime is also characterized by large cyclic variations. Beyond cycle 300, when the fuel was turned off, the LII signal did not immediately disappear. This may be from residual soot in the exhaust flow, but more likely is due to LII from soot deposits on the windows. We have confirmed that the background LII signal is not from thermal emissions emanating directly from the fouled windows; rather, it is LII from soot particles in the probe volume created by condensation of vaporized soot from the windows.

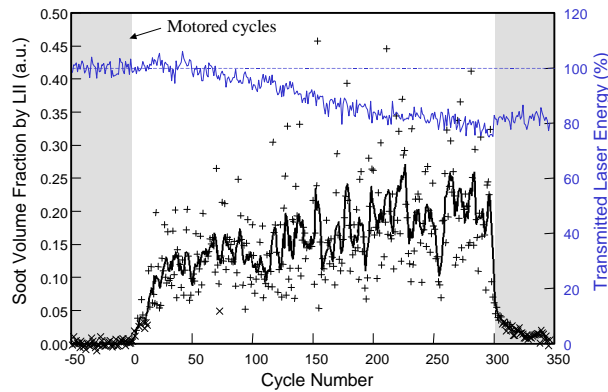


Fig. 8 LII and laser transmission measurements for open-valve injection during a simulated cold start. (Symbols as defined in Fig. 7.)

At the top of Fig. 8 we show the transmitted laser energy through the two opposed windows, normalized by the average energy measured during the 50 motored cycles at the beginning of the test. It is seen to decay nearly linearly with time, starting from about cycle 50. At the end of the fueled period, the transmitted energy jumps suddenly to a higher, constant value. This jump may be from a gain in transmittance through the exhaust flow, but also may be due to continued vaporization of soot deposits on the windows.

The corresponding measurements for closed-valve injection are presented in Fig. 9. Unlike the open-valve injection data, there is a spike in the LII signal at the onset of combustion, followed by a near-linear decay for the remainder of the test sequence. However, there also is a very strange behavior to the background LII signal. For Fig. 8, the background level was calculated as the average of the first group of motored cycles (-50-0), while for this case it was calculated from the last group of motored cycles (300-350). This was necessary because the background LII signal dropped significantly with the onset of combustion - it was 0.050 during the first motored group, and 0.030 during the last group. If the former, larger value had been subtracted from the raw data, the LII measurements for cycles beyond 50 would be negative. In fact, even a linear interpolation between these two values results in negative LII values between cycles 50 and 250. This is because the background LII signal changes quickly at the onset of combustion, rather than changing slowly throughout the combustion period. Despite this uncertainty in the background level, it can still be concluded that the soot concentration with closed-valve injection is considerable less after 50 engine cycles when compared with open-valve injection.

At least part of the explanation for this strange behavior can be found in the measurements of transmitted laser energy, which show an abrupt increase of about 10% at the onset of combustion. The most plausible explanation for this increase is that whatever caused the spike in the LII signal also caused significant steering or blooming of the laser beam. This would result in va-

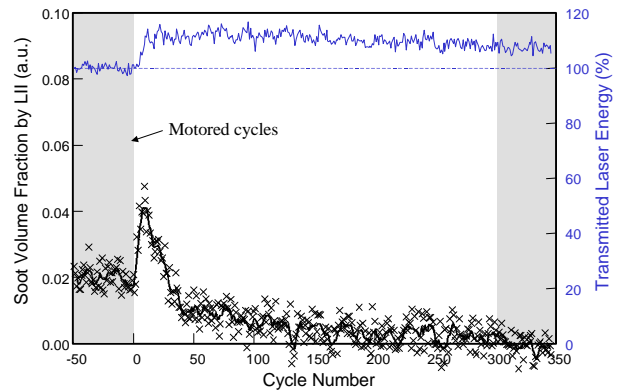


Fig. 9 LII and laser transmission measurements for closed-valve injection during a simulated cold start. (Symbols as defined in Fig. 7.)

porization of soot from the exit window in areas that formerly were attenuating the beam and the source of background LII.

LII DURING SNAP-THROTTLE

As mentioned earlier, the unrealistic rich mixture used in these first tests was selected to assure that we had measurable concentrations of soot during the learning phase of this research. For a final, realistic demonstration of the LII technique, we chose to perform a very rapid load transient, as illustrated in Fig. 10. The snap-throttle test started with the same simulated cold start, except that a stoichiometric mixture was used. After 150 cycles, a large solenoid valve was rapidly opened to bring the intake manifold to ambient pressure. The measurements in Fig. 10 are for motored operation, to show how quickly the manifold and cylinder pressure reach the wide-open-throttle (WOT) condition.

At the time of the throttle change, the fueling duration was also increased to maintain stoichiometric input conditions; open-valve injection was used. We used a universal exhaust gas oxygen sensor (UEGO) to measure the in-cylinder mixture equivalence ratio, as shown in Fig. 11. Although the temporal response of the UEGO is known to be marginal, these results confirm that the mixture was stoichiometric by the time of the throttle change and the end of the WOT period. As is clearly seen in the measurements, the electronics for this particular UEGO cause wild oscillations when the mixture is stoichiometric. This behavior is contrary to that reported by Cornelius, et al.[25], who observed a spike only when crossing from lean to rich. Note also that the snap-throttle resulted in a misfire, which is interpreted by the UEGO as an ultra lean cycle because of the excess oxygen.

Finally, shown in Fig. 12 are LII measurements made during the snap throttle, along with laser beam transmission data. Similar to the behavior during cold start, there is no abrupt appearance of soot at the time of the snap-throttle. Instead, the soot volume fraction actually falls to zero for the first 20 cycles, after which there again is a slow, steady increase in soot as the test pro-

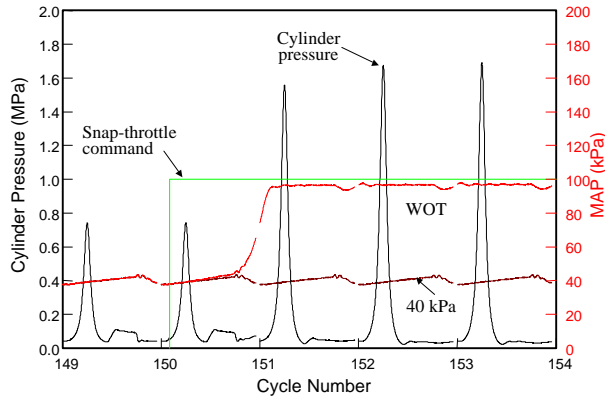


Fig. 10 Intake manifold and cylinder pressures during a motored snap-throttle.

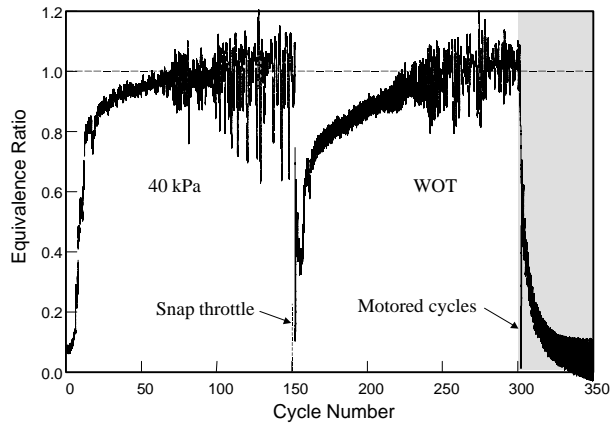


Fig. 11 UEGO measurements of the equivalence ratio during the snap-throttle sequence.

gresses. By the end of the sequence, the soot volume fraction for WOT, $\phi=1.0$, is about twice that shown in Fig. 8 for 40 kPa, $\phi=1.24$.

The attenuation of the laser beam is also severe; if it is assumed that half of the attenuation occurs at the exit window, there still is a 20% loss in incident laser energy into the LII probe volume. This, of course, affects the final temperature of the laser-heated soot particles which, in turn, affects the amplitude of the LII signal. Contrary to the often-cited model of LII signals being constant above a threshold laser-fluence level of about 0.2 J/cm^2 , laser-induced vaporization can have a significant effect on signal levels [22]. As mentioned earlier, the increase in transmission when combustion stopped can be due to either less extinction through the exhaust gas or cleaner windows from laser vaporization of soot deposits.

CONCLUSIONS

The purpose of this paper is to demonstrate the capability of LII for making time-resolved measurements of soot volume fraction during engine transients. LII measurements are essentially instantaneous, obtained in just a few 10's of nanoseconds. The achievable time-resolution, however, is limited by the repetition rate of a high-energy pulsed laser, which is typically 10-30 Hz. The minimum laser fluence is about 0.2 J/cm^2 , and this

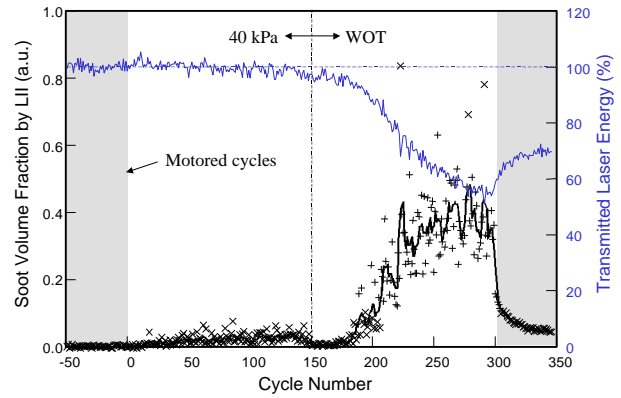


Fig. 12 LII and laser transmission measurements during the snap-throttle sequence. (Symbols as defined in Fig. 7.)

cannot be achieved by focusing a continuous-wave laser beam because the LII probe volume dimensions need to be on the order of millimeters for single-shot measurements to be possible. Thus, the technique is inherently limited to just a few measurements during an engine cycle. This allows three modes of time-resolved applications: 1) Cycle-resolved, real-time transients, where measurements are made at a single, fixed crank-angle position for successive engine cycles (as demonstrated in Figs. 8, 9, and 12); 2) Ensemble-averaged, crank-angle-resolved measurements of inter-cycle transients during steady-state operation, where measurements are made at incremental crank-angle positions for successive engine cycles (as simulated in Fig. 7); 3) Ensemble-averaged, crank-angle-resolved measurements of repeated transients, where measurements are made at incremented crank-angle positions for successive engine cycles and multiple repetitions of a transient test sequence (as demonstrated by Green [26]).

The limiting factor in the practicality of LII measurements of engine exhaust is the problem of window fouling. We believe that an active approach using a clean-gas flow to isolate windows from the exhaust flow is essential. While this adds complexity to the instrument, it is not a significant liability.

Planar LII images made in the exhaust port show that soot concentration varies widely both spatially and temporally, from cycle-to-cycle. For some cycles the soot distribution was relatively uniform, whereas for others it varied greatly between the two valves. On average, the amount of soot emitted from the two valves was significantly different.

For open-valve injection the soot volume fraction was shown to increase rapidly over the first 20 cycles of a simulated cold start, and then continue to increase at a slower rate for the duration of the 300 cycle test. In contrast, for closed-valve injection the soot volume fraction rose very quickly to a maximum in less than 10 cycles, and then fell rapidly to a low concentration by about 50 cycles, after which it continued to fall gradually for the remainder of the test. We believe the large differences in the soot behavior for these two cases is related to the dynamics of the in-cylinder wall films,

and in particular to the changing composition of the films as the wall temperatures increase.

For a snap-throttle from 40 to 98 kPa MAP, the soot volume fraction increased steadily during the throttled period, fell to near zero at the time of the snap-throttle, and then increased steadily to a value approximately ten times greater than for the throttled period. Severe window fouling occurred during the WOT portion of this test, resulting in a 30% loss in laser beam transmission after engine shutdown.

Acknowledgements

This work was performed at the Combustion Research Facility of the Sandia National Laboratories, and was funded by the U.S. Department of Energy, Office of Transportation Technologies, Office of Advanced Automotive Technologies under the direction of Kathi Epping and Rogelio Sullivan. The author is particularly thankful to Robert Green and Hope Michelsen for their helpful comments and review of this manuscript.

REFERENCES

- [1] Quader, A. A., "How Injector, Engine, and Fuel Variables Impact Smoke and Hydrocarbon Emissions with Port Fuel Injection," *Trans. SAE* **98**, Sec. 4, p. 327, 1989.
- [2] Kosowski, M. G., "Soot Formation in a Multipoint-Fuel-Injected Spark-Ignited Engine," *Trans. SAE* **94**, Sec. 2, p. 786, 1985.
- [3] Lawson, D. R. and Smith, R. E., "The Northern Front Range Air Quality Study: A Report to the Governor and General Assembly," Colorado State University, December, 1998.
- [4] Baumgard, K. J. and Johnson, J. H., "The Effect of Fuel and Engine Design on Diesel Exhaust Particle Size Distributions," SAE Paper No. 960131, 1996.
- [5] Witze, P. O. and Green, R. M., "LIF and Flame-Emission Imaging of Liquid Fuel Films and Pool Fires in an SI Engine During a Simulated Cold Start," SAE Paper No. 970866, 1997.
- [6] Nogi, T., Ohyama, Y., Yamauchi, T. and Kuroiwa, H., "Mixture Formation of Fuel Injection Systems in Gasoline Engines," SAE Paper No. 880558, 1988.
- [7] Nogi, T., Ohyama, Y. and Yamauchi, T., "Effects of Mixture Formation of Fuel Injection Systems in Gasoline Engine," SAE Paper No. 891961, 1989.
- [8] Ohyama, Y., Ohsuga, M. and Kuroiwa, H., "Study of Mixture Formation and Ignition Process in Spark Ignition Engine Using Optical Combustion Sensor," *Trans. SAE*, **99**, Sec. 3, p. 2002, 1990.
- [9] Ohyama, Y., Nogi, T. and Ohsuga, M., "Effects of Fuel/Air Mixture Preparation on Fuel Consumption and Exhaust Emission in a Spark Ignition Engine," IMech E Paper C389/232, p. 59, 1992.
- [10] Song, K., Clasen, E., Chang, C., Campbell, S. and Rhee, K. T., "Post-Flame Oxidation and Unburned Hydrocarbon in a Spark-Ignition Engine," SAE Paper 952543, 1995.
- [11] Stevens, E. and Steeper, R., "Piston Wetting in an Optical DISI Engine: Fuel Films, Pool Fires, and Soot Generation," SAE Paper No. 2001-01-1203, 2001.
- [12] Kayes, D. and Hochgreb, S., "Mechanisms of Particulate Matter Formation in Spark-Ignition Engines. 3. Model of PM Formation," *Environmental Science and Technology* **33**, pp. 3978-3992, 1999.
- [13] Kayes, D., Liu, H. and Hochgreb, S., "Particulate Matter Emission During Start-up and Transient Operation of a Spark-Ignition Engine," SAE Paper No. 1999-01-3529, 1999.
- [14] Vander Wal, R. L. and Weiland, K. J., "Laser-Induced Incandescence: Development and Characterization Towards a Measurement of Soot Volume Fraction," *Applied Physics B* **59**, pp. 445-452, 1994.
- [15] Shaddix, C. R. and Smyth, K. C., "Quantitative Measurements of Enhanced Soot Production in Steady and Flickering Methane/Air Diffusion Flame," *Combustion & Flame* **99**, pp. 723-732, 1994.
- [16] Ni, T., Pinson, J. A., Gupta, S. and Santoro, R. J., "Two-Dimensional Imaging of Soot Volume Fraction by the Use of Laser-Induced Incandescence," *Applied Optics* **34**, No. 30, pp. 7083-7091, 1995.
- [17] Dec., J. E., zur Loye, A. O. and Siebers, D. L., "Soot Distribution in a D. I. Diesel Engine Using 2-D Laser-Induced Incandescence Imaging," SAE Paper No. 910224, 1991.
- [18] Won, Y-H., Kamimoto, T., Kobayashi, H. and Kosaka, H., "2-D Soot Visualization in Unsteady Spray Flame by means of Laser Sheet Scattering Technique," SAE Paper No. 910223, 1991.
- [19] Pinson, J. A., Mitchell, D. L., Santoro, R. J. and Litzinger, T. A., "Quantitative, Planar Soot Measurements in a D.I. Diesel Engine Using Laser-Induced Incandescence and Light Scattering," SAE Paper No. 932650, 1993.
- [20] Wainner, R. T., Seitzman, J. M. and Martin, S. R., "Soot Measurements in a Simulated Engine Exhaust using Laser-Induced Incandescence," *AIAA J.* **37**, No. 6, pp. 738-743, 1999.
- [21] Eckbreth, A. C., "Effects of Laser-Modulated Particulate Incandescence on Raman Scattering Diagnostics," *J. Applied Physics* **48**, No. 11, pp. 4473-4479, 1977.
- [22] Witze, P. O., Hochgreb, S., Kayes, D., Michelsen, H. A. and Shaddix, C. R., "Time-Resolved Laser-Induced Incandescence and Laser Elastic Scattering Measurements in a Propane Diffusion Flame," to appear in *Applied Optics*, 2001.
- [23] Vander Wal, R. L. and Choi, M. Y., "Pulsed Laser Heating of Soot: Morphological Changes," *Carbon* **37**, No. 2, pp. 231-239, 1999.
- [24] Fox, J. W., Min, K. D., Cheng, W. K. and Heywood, J. B., "Mixture Preparation in a SI Engine with Port Fuel Injection During Starting and Warm-Up," SAE Paper 922170, 1992.
- [25] Cornelius, S. J., Davison, D. E., Collings, N., and Glover, K., "Observations of Trans-Stoichiometric AFR Spikes in UEGO Sensors," SAE Paper 2000-01-2837, 2000.
- [26] Green, R. M., "Measuring the Cylinder-to-Cylinder EGR Distribution in the Intake of a Diesel Engine During Transient Operation," SAE Paper 2000-01-2866, 2000.